Joint Active Precoding for RIS-aided Cell-free MIMO Networks

Ghadir Dogim
German University in Cairo
ghader.mahmoud@guc.edu.eg

Engy Aly Maher
German University in Cairo
engy.aly@guc.edu.eg

Ahmed El-Mahdy
German University in Cairo
ahmed.elmahdy@guc.edu.eg

Falko Dressler
TU Berlin
dressler@ccs-labs.org

***Abstract*—In the future communications, cell-free networks are considered very promising, owing to their robustness against inter-cell interference which degrades the user signal-to-interference-plus-noise-ratio (SINR). For an efficient network to achieve an enhanced capacity at a minimized power consumption, reconfigurable intelligent surfaces (RIS) are promoted as a key candidate 6G technology. In this paper, a joint precoding RIS aided cell-free Multiple-Input-Multiple-Output (MIMO) network is considered, where a weighted sum rate (WSR) maximization problem is formulated and decoupled into subproblems. A feasible solution is then obtained using fractional programming (FP). Finally, the performance of passive RIS and active RIS is then compared.**

***Index Terms*—Cell-free MIMO, Reconfigurable intelligent surfaces, Active-RIS, Joint precoding, Multiplicative fading, Fractional Programing, Quadratic constraint quadratic programming**

I. Introduction

Cell-free (CF) massive MIMO has been introduced [1], in which many geographically distributed access points (APs) jointly and coherently serve the network users without cellular boundaries. The APs efficiently cooperate through backhaul links and a CPU, which allows them to operate simultaneously [2]. Accordingly, the inter-cell interference can be mitigated by coherent cooperation between the distributed APs [3]. In beyond 6G networks, RISs have been introduced as a supplementary cost-effective addition to existing networks [4].

Passive RISs are recently employed in CF networks to reduce the number of used APs. However, multiplicative fading is a limiting factor which leads to a negligible performance gain in terms of the spectral efficiency of CF-MIMO networks, as studied in [5]. This motivated us to use active RISs in CF-MIMO networks, owing to their ability to mitigate multiplicative fading and overcome this limitation. The reflecting amplifiers installed aim to amplify the signal and apply phase adjustment prior to reflection. Accordingly, a performance enhancement in terms of spectral efficiency and network coverage can be achieved. Moreover, the significance of the performance gain over passive RISs and whether it is still maintained when multiple active RISs are considered are crucial aspects that we aim to investigate.

This work is supported by the DAAD and in part by the Federal Ministry of Education and Research (BMBF, Germany) within the 6G Research and Innovation Cluster 6G-RIC under Grant 16KISK020K, in co-operation between TU Berlin and the German University in Cairo

II. Related work

In [5], the authors aggregate passive RISs to CF networks, by replacing some of the base stations (BSs) by passive RISs. A joint precoding design at BSs and passive RIS was formulated and solved using fractional programming (FP). However, the simulation results demonstrate that, passive RISs introduce a negligible performance gain.

In [6], the authors integrate passive RISs to a CF network. A channel estimation scheme is then proposed, aiming to minimize the overhead load introduced by channel estimation of individual RIS elements. The RIS phase shifts are optimized based on statistical channel state information (CSI) to enhance the performance of both, uplink and downlink transmission phases for single antenna users and BSs.

In [7], the authors consider an active RIS-aided CF network, to enhance the capacity. Multiple active RISs assist the uplink transmission of single antenna users. Moreover, a Joint Beamforming and Resource Allocation (JBRA) optimization algorithm is proposed, to maximize the worst user's energy efficiency (EE). However, the overall spectral energy of all the network users over the downlink was not tackled.

Unlike our counterparts from the literature, our main focus is to consider active RISs in a CF-MIMO network, were the users and APs are both equipped with multiple antennas, to maximize the WSR of all the network users. On the contrary, previous work either considered passive RIS in CF-MIMO networks which lead to an insignificant performance gain or maximizing EE of individual users which focuses on the fairness rather than the overall network performance. Our main contributions can be summarized as follows:

- Considering active RISs in a multi-user CF-MIMO network for multiple antenna users and APs.
- For a downlink communication setup, the user SINR expressions are derived and a WSR maximization problem is formulated, subject to APs and RIS transmission power constraints to jointly optimize the active precoders at both the APs and RIS.
- Investigating the effectiveness of active RIS in terms of mitigating the multiplicative fading effect for multi-user CF-MIMO networks.

III. System Model

A CF network is implemented as shown in Fig. 1, with B APs equipped with M antennas each and R RIS, composed of

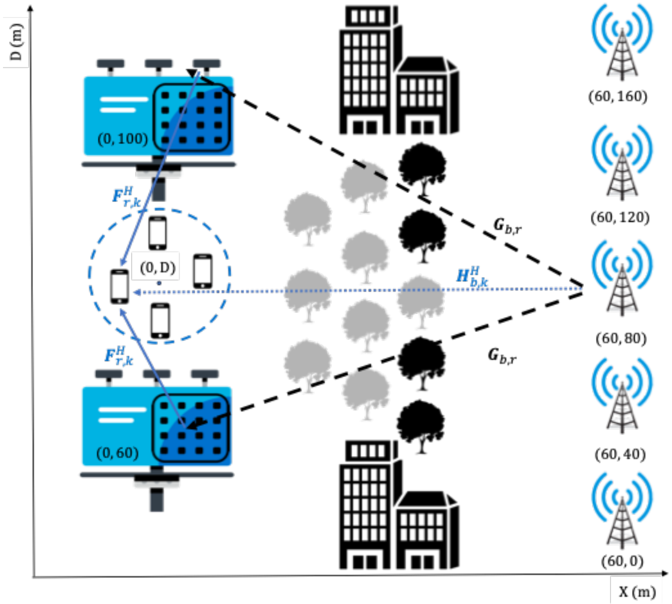

Fig. 1. CF-MIMO system model. Two scenarios are considered, when the direct link between the APs and the users is either premitted or completely blocked.

N elements each. The APs and RIS are connected through a wireless backhaul link to a single central processing unit [8]. Thus, they are implemented to jointly and coherently serve K users equipped with U antennas each, uniformly distributed over a circle of radius R_D, centered at $(0, D)$. Moreover, the index sets are denoted by $\mathcal{B} = \{1, \ldots, B\}$, $\mathcal{R} = \{1, \ldots, R\}$, $\mathcal{N} = \{1, \ldots, N\}$, $\mathcal{K} = \{1, \ldots, K\}$ for the APs, RIS, RIS elements and users, respectively. The symbol precoded by the b^{th} AP can be denoted by:

$$\mathbf{x}_b = \sum_{j=1}^{K} \mathbf{w}_{b,j} \mathbf{s}_j \tag{1}$$

where $\mathbf{s} \triangleq [\mathbf{s}_1, \ldots, \mathbf{s}_K] \in \mathbb{C}^K$ denotes the normalized power transmitted symbol for the K users, i.e., $\mathbb{E}\{\mathbf{s}\mathbf{s}^H\} = \mathbf{I}_K$. Additionally $\mathbf{w}_{b,k} \in \mathbb{C}^K$ denotes the precoding vector of the b^{th} AP. The signal received by each user is a superposition of the signals transmitted by the APs through their direct link (DL) with the user and the signals reflected and amplified by the active RIS. Accordingly, the composite channel $\mathbf{h}^H_{b,k} \in \mathbb{C}^{U \times M}$ from b^{th} AP to k^{th} user can be expressed as:

$$\mathbf{h}^H_{b,k} = \mathbf{H}^H_{b,k} + \sum_{r=1}^{R} \mathbf{F}^H_{r,k} \mathbf{P}_r \boldsymbol{\Theta}^H_r \mathbf{G}_{b,r} \tag{2}$$

The Rician fading channel model in [9] is implemented, where $\mathbf{H}^H_{b,k} \in \mathbb{C}^{U \times M}, \mathbf{G}_{b,r} \in \mathbb{C}^{N \times M}, \mathbf{F}^H_{r,k} \in \mathbb{C}^{U \times N}$ are the frequency domain channels between b^{th} AP and k^{th} user, r^{th} RIS and k^{th} user and b^{th} AP and r^{th} RIS, respectively. Moreover, $\mathbf{P}_r = \text{diag}\left(p_1, p_2, \ldots, p_N\right)$ and $\boldsymbol{\Theta}^H_r = \text{diag}\left(e^{j\theta_1}, e^{j\theta_2}, \ldots, e^{j\theta_N}\right)$ are the amplification and phase shift matrices for each r^{th} RIS, respectively. $\mathbf{P}_r$ and $\boldsymbol{\Theta}_r$ will always appear in the product form, thus they can be merged together into one variable, denoted by $\boldsymbol{\Psi}_r$, where $\boldsymbol{\Psi}_r = \mathbf{P}_r \boldsymbol{\Theta}_r = \text{diag}\left(p_1 e^{j\theta_1}, p_2 e^{j\theta_2}, \ldots, p_N e^{j\theta_N}\right)$.

IV. Weighted Sum Rate Optimization Problem

The received signal at k^{th} user from b^{th} AP denoted by $\mathbf{y}_{b,k} \in \mathbb{C}^U$ can be represented by:

$$\mathbf{y}_{b,k} = \mathbf{h}^H_{b,k} \mathbf{x}_b = \left(\mathbf{H}^H_{b,k} + \sum_{r=1}^{R} \mathbf{F}^H_{r,k} \boldsymbol{\Psi}^H_r \mathbf{G}_{b,r} \right) \sum_{j=1}^{K} \mathbf{w}_{b,j} \mathbf{s}_j \tag{3}$$

Accordingly, the equivalent signal received by k^{th} user from all APs can be represented by (4), given at the top of the next page, where $\mathbf{z}_k \triangleq [z^T_{k,1}, \ldots, z^T_{k,U}]^T$ is the additive white Gaussian noise (AWGN) with covariance $\mathbf{z}_k \sim \mathcal{CN}(\mathbf{0}_U, \boldsymbol{\Xi}_K)$, where $\boldsymbol{\Xi}_K = \sigma^2_n \mathbf{I}_U$. By defining $\boldsymbol{\Psi} = \text{diag}\left(\boldsymbol{\Psi}_1, \boldsymbol{\Psi}_2, \ldots, \boldsymbol{\Psi}_R\right), \mathbf{F}_k = [\mathbf{F}^T_{1,k}, \ldots, \mathbf{F}^T_{R,k}]^T, \mathbf{G}_b = [\mathbf{G}^T_{b,1}, \ldots, \mathbf{G}^T_{b,R}]^T, \mathbf{h}_k = [\mathbf{h}^T_{1,k}, \ldots, \mathbf{h}^T_{B,k}]^T$, and $\mathbf{w}_k = [\mathbf{w}^T_{1,k}, \ldots, \mathbf{w}^T_{B,k}]^T$. Thus, $\mathbf{y}_k$ in (4) can be reformulated as:

$$\mathbf{y}_k = \sum_{j=1}^{K} \mathbf{h}^H_k \mathbf{w}_j \mathbf{s}_j + \mathbf{F}^H_k \boldsymbol{\Psi}^H \mathbf{v} + \mathbf{z}_k \tag{5}$$

where $\mathbf{v} = [\mathbf{v}^T_1, \ \mathbf{v}^T_2, \ \ldots \ \mathbf{v}^T_R]^T$, such that $\mathbf{v}_r \sim \mathcal{CN}(\mathbf{0}_N, \sigma_{v^2} \, \mathbf{I}_N)$ is the dynamic noise influenced by devices of the active RIS elements [10].

Using (4), the user SINR denoted by γ_k is represented by (6), at the top of the next page. Finally, the WSR is given by:

$$\mathcal{R}_1(\boldsymbol{\Psi}, \mathbf{W}) = \sum_{k=1}^{K} \eta_k \log_2(1 + \gamma_k) \tag{7}$$

where $\eta_k \in \mathbb{R}^+$ denotes the weight for k^{th} user. Accordingly, the WSR maximization problem can be formulated as:

$$\mathcal{P}_0: \max_{\mathrm{P}, \boldsymbol{\Theta}, \mathrm{W}} \quad \mathcal{R}_1(\boldsymbol{\Psi}, \mathbf{W}) \tag{8a}$$

$$\text{s.t.} \quad \text{C1}: \sum_{j=1}^{K} \|\mathbf{w}_{b,j}\|^2 \leq \mathrm{P_b}, \qquad \forall b \in \mathcal{B} \tag{8b}$$

$$\text{C2}: \sum_{b=1}^{B} \sum_{j=1}^{K} \|\boldsymbol{\Psi}^H_r \mathbf{G}_{b,r} \mathbf{w}_{b,j}\|^2 + \|\boldsymbol{\Psi}^H_r \mathbf{v}_r\|^2 \leq \mathrm{P_R}, \quad \forall r \in \mathcal{R} \tag{8c}$$

where $\mathrm{P_b}$ and $\mathrm{P_R}$ denote the maximum transmission powers for each AP and all RIS, respectively and $\mathbf{W} = [\mathbf{w}^T_1, \ldots, \mathbf{w}^T_K]^T$ is the composite APs to users precoding matrix. Since problem $\mathcal{P}_0$ is non-convex, we implement a modified version of the joint precoding frameworks, using fractional programming (FP) [11].

V. Joint AP transmission beamforming and Active RIS precoding algorithm

In this section, we present the proposed methodology to solve the WSR maximization problem in (8), which can be solved by finding a feasible solution for $\boldsymbol{\Psi}^{\text{opt}}$ and $\mathbf{W}^{\text{opt}}$.

$$
\begin{aligned}
\mathbf{y}_k &= \sum_{b=1}^{B} \mathbf{y}_{b,k} + \mathbf{z}_k = \sum_{b=1}^{B} \left(\mathbf{H}_{b,k}^H + \sum_{r=1}^{R} \mathbf{F}_{r,k}^H \boldsymbol{\Psi}_r^H \mathbf{G}_{b,r} \right) \sum_{j=1}^{K} \mathbf{w}_{b,j} \mathbf{s}_j + \sum_{r=1}^{R} \mathbf{F}_{r,k}^H \mathbf{P}_r \boldsymbol{\Theta}_r^H \mathbf{v}_r + \mathbf{z}_k \\
&= \underbrace{\sum_{b=1}^{B} \left(\mathbf{H}_{b,k}^H + \sum_{r=1}^{R} \mathbf{F}_{r,k}^H \boldsymbol{\Psi}_r^H \mathbf{G}_{b,r} \right) \mathbf{w}_{b,k} \mathbf{s}_k}_{\textbf{Desired signal to user } k} + \underbrace{\sum_{b=1}^{B} \left(\mathbf{H}_{b,k}^H + \sum_{r=1}^{R} \mathbf{F}_{r,k}^H \boldsymbol{\Psi}_r^H \mathbf{G}_{b,r} \right) \sum_{\substack{j=1 \\ j \neq k}}^{K} \mathbf{w}_{b,j} \mathbf{s}_j}_{\textbf{Interference from other users}} \\
&\quad + \underbrace{\sum_{r=1}^{R} \mathbf{F}_{r,k}^H \boldsymbol{\Psi}_r^H \mathbf{v}_r}_{\textbf{Noise amplified by active RIS}} + \underbrace{\mathbf{z}_k}_{\textbf{AWGN}}
\end{aligned} \tag{4}
$$

$$
\gamma_k = \mathbf{w}_k^H \mathbf{h}_k \left(\sum_{j=1}^{K} \mathbf{h}_k^H \mathbf{w}_j \left(\mathbf{h}_k^H \mathbf{w}_j \right)^H + \boldsymbol{\Xi}_k + \sigma_n^2 \mathbf{F}_k^H \boldsymbol{\Psi}^H \left(\mathbf{F}_k^H \boldsymbol{\Psi}^H \right)^H \right)^{-1} \mathbf{h}_k^H \mathbf{w}_k \tag{6}
$$

A. Lagrangian Dual Reformulation (LDR) and Multi-dimensional Complex Quadratic Transform (MCQT)

LDR [11] is used to segregate the sum of logarithms in problem $\mathcal{P}_0$, given by (8). By introducing the first auxiliary variable $\boldsymbol{\rho} \triangleq [\rho_1, \rho_2, \ldots, \rho_K]$, $\mathcal{R}_1(\boldsymbol{\Psi}, \mathbf{W})$ of problem $\mathcal{P}_0$ in (8) can be reformulated as:

$$
\begin{aligned}
\mathcal{R}_2(\boldsymbol{\Psi}, \mathbf{W}, \boldsymbol{\rho}) &= \sum_{k=1}^{K} \eta_k \ln(1+\rho_k) - \sum_{k=1}^{K} \eta_k \boldsymbol{\rho}_k \\
&\quad + \sum_{k=1}^{K} f_k \left(\boldsymbol{\Psi}, \mathbf{W}, \boldsymbol{\rho} \right)
\end{aligned} \tag{9}
$$

where $f_k \left(\boldsymbol{\Psi}, \mathbf{W}, \boldsymbol{\rho} \right)$ is given by (10), at the top of the next page. $f_k \left(\boldsymbol{\Psi}, \mathbf{W} \right)$ is high dimensional and non-convex due to the products of matrices and inverse matrices of the RIS channels. Thereby, its non-convexity of cannot be relaxed by adopting the common FP methods such as the Dinkelbach's algorithms [12]. Thus, since (10) meets the concave-convex conditions required, MCQT be adopted since it extends the common scalar-form FP to a matrix-form to resolve the non-convexity of high-dimensional fractions of matrices. Accordingly, $f_k \left(\boldsymbol{\Psi}, \mathbf{W} \right)$ in (10) can be equivalently reformulated as $\mathbf{g}_k \left(\boldsymbol{\Psi}, \mathbf{W}, \boldsymbol{\rho}, \boldsymbol{\varpi} \right)$, defined by (11), given at the top of the next page, where $\boldsymbol{\varpi} \triangleq [\boldsymbol{\varpi}_1, \boldsymbol{\varpi}_2, \ldots, \boldsymbol{\varpi}_K]$ is a second auxiliary variable, to be optimized and $\mu_k = \sqrt{\eta_k(1+\rho_k)}$. Finally, using (9) and (11), problem $\mathcal{P}_0$ can be reformulated into problem $\mathcal{P}_1$ given by:

$$
\begin{aligned}
\mathcal{P}_1\colon \quad & \max_{\boldsymbol{\Psi}, \mathbf{W}, \boldsymbol{\rho}, \boldsymbol{\varpi}} \quad \mathcal{R}_2(\boldsymbol{\Psi}, \mathbf{W}, \boldsymbol{\rho}, \boldsymbol{\varpi}) \\
\text{s.t.} \quad & \mathrm{C1}, \mathrm{C2}
\end{aligned} \tag{12}
$$

Accordingly, a local optimal solution is found by dividing problem $\mathcal{P}_1$ into four subproblems, by fixing three variables and optimizing the fourth. Thus, alternately optimizing $\boldsymbol{\Psi}, \mathbf{W}, \boldsymbol{\rho}$ and $\boldsymbol{\varpi}$ until $\mathcal{R}_2$ converges.

B. Fixing $(\boldsymbol{\Psi}, \mathbf{W}, \boldsymbol{\varpi})$ and optimizing $\boldsymbol{\rho}$:

By solving $\frac{\partial \mathcal{R}_2(\boldsymbol{\Psi}, \mathbf{W}, \boldsymbol{\rho}, \boldsymbol{\varpi})}{\partial \rho_k} = 0$, ρ_k can be obtained by:

$$
\rho_k^{\text{opt}} = \gamma_k^* = \frac{\xi_k^2 + \xi_k \sqrt{\xi_k^2 + 4\eta_k}}{2\eta_k}, \qquad \forall k \in \{1, \ldots, \mathcal{K}\} \tag{13}
$$

where $\xi_k = \mathbb{R}\{\boldsymbol{\varpi}_k^H \mathbf{h}_k \mathbf{w}_k\}$.

C. Fixing $(\boldsymbol{\Psi}, \mathbf{W}, \boldsymbol{\rho})$ and optimizing $\boldsymbol{\varpi}$:

By using the derivative of quadratic functions, and the product rule in their matrix form, solving $\frac{\partial \mathcal{R}_2(\boldsymbol{\Psi}, \mathbf{W}, \boldsymbol{\rho}, \boldsymbol{\varpi})}{\partial \boldsymbol{\varpi}_k} = 0$ it results in:

$$
\boldsymbol{\varpi}_k^H = \frac{\mu_k \mathbb{R}\{\mathbf{h}_k \mathbf{w}_k\}}{\sum_{j=1}^{K} \mathbf{h}_k \mathbf{w}_j \left(\mathbf{h}_k \mathbf{w}_j \right)^H + \boldsymbol{\Xi}_k + \sigma_n^2 \mathbf{F}_k^H \boldsymbol{\Psi}^H \boldsymbol{\Psi} \mathbf{F}_k} \tag{14}
$$

D. Fixing $(\boldsymbol{\Psi}, \boldsymbol{\rho}, \boldsymbol{\varpi})$ and optimizing $\mathbf{W}$:

The following definitions are first introduced to simplify the notations of the joint precoding algorithm, let:

$$
\mathbf{c}_k = \mu_k \{\mathbf{h}_k \boldsymbol{\varpi}_k^H\}, \ \mathbf{C} = \left[\mathbf{c}_1^T, \mathbf{c}_2^T, \ldots, \mathbf{c}_K^T \right] \tag{16a}
$$

$$
\mathbf{a}_k = \sum_{j=1}^{K} \mathbf{h}_k \boldsymbol{\varpi}_k \left(\mathbf{h}_k \boldsymbol{\varpi}_k \right)^H, \quad \mathbf{A} = \mathbf{I}_K \otimes \mathbf{a}_k \tag{16b}
$$

$$
\mathbf{Y} = \sum_{k=1}^{K} \boldsymbol{\varpi}_k^H \left(\boldsymbol{\Xi}_k + \sigma_n^2 \, \mathbf{F}_k^H \boldsymbol{\Psi}_r^H \left(\mathbf{F}_k^H \boldsymbol{\Psi}_r^H \right)^H \right) \boldsymbol{\varpi}_k \tag{16c}
$$

$$
\mathrm{P_m} = \mathrm{P_R} - \sigma_n^2 \|\boldsymbol{\Psi}_r\|^2 \tag{16d}
$$

Using the above definitions, for a fixed RIS precoding matrix $\boldsymbol{\Psi}$, auxilliary variables $\boldsymbol{\rho}$ and $\boldsymbol{\varpi}$, problem $\mathcal{P}_1$ in (12) can be reformulated as:

$$
\begin{aligned}
\mathcal{P}_2\colon \quad & \max_{\mathbf{W}} \quad \mathbb{R}\{2\, \mathbf{C}^H \mathbf{W}\} - \mathbf{W}^H \mathbf{A} \mathbf{W} - \mathbf{Y} \\
\text{s.t.} \quad & \mathrm{C1}\colon \mathbf{W}^H \mathbf{D}_b \mathbf{W} \le \mathrm{P_b} \\
& \mathrm{C2}\colon \mathbf{W}^H \mathbf{Z} \mathbf{W} \le \mathrm{P_m}
\end{aligned} \tag{17}
$$

$$f_k\left(\mathbf{\Psi},\mathbf{W},\boldsymbol{\rho}\right)=\eta_k(1+\rho_k)\mathbf{w}_k^H\mathbf{h}_k\left(\sum_{j=1}^{K}\mathbf{h}_k^H\mathbf{w}_j\left(\mathbf{h}_k^H\mathbf{w}_j\right)^H+\mathbf{\Xi}_k+\sigma_n^2\mathbf{F}_k^H\mathbf{\Psi}^H\left(\mathbf{F}_k^H\mathbf{\Psi}^H\right)^H\right)^{-1}\mathbf{h}_k^H\mathbf{w}_k \tag{10}$$

$$\mathbf{g}_k\left(\mathbf{\Psi},\mathbf{W},\boldsymbol{\rho},\boldsymbol{\varpi}\right)=2\mu_k\mathbb{R}\{\boldsymbol{\varpi}_k^H\mathbf{h}_k\mathbf{w}_k\}-\sum_{k=1}^{K}\boldsymbol{\varpi}_k^H\left[\sum_{j=1}^{K}\mathbf{h}_k\mathbf{w}_j\left(\mathbf{h}_k\mathbf{w}_j\right)^H+\mathbf{\Xi}_k+\sigma_n^2\mathbf{F}_k^H\mathbf{\Psi}^H\left(\mathbf{F}_k^H\mathbf{\Psi}^H\right)^H\right]\boldsymbol{\varpi}_k \tag{11}$$

$$\begin{aligned}&\mathbf{q}_k\left(\mathbf{\Psi},\mathbf{W},\ \boldsymbol{\rho},\ \boldsymbol{\varpi}\right)=2\mu_k\ \mathbb{R}\{\boldsymbol{\varpi}_k^H\ \sum_{b=1}^{B}\left(\mathbf{H}_{b,k}^H+\mathbf{F}_k^H\ \mathbf{\Psi}^H\ \mathbf{G}_b\right)\mathbf{w}_{b,k}\}\\&-\sum_{k=1}^{K}\boldsymbol{\varpi}_k^H\left\langle\sum_{b=1}^{B}\left[\left(\mathbf{H}_{b,k}^H+\mathbf{F}_k^H\ \mathbf{\Psi}^H\ \mathbf{G}_b\right)\sum_{j=1}^{K}\left(\mathbf{w}_{b,j}\mathbf{w}_{b,j}^H\right)\left(\mathbf{H}_{b,k}^H+\mathbf{F}_k^H\ \mathbf{\Psi}^H\ \mathbf{G}_b\right)^H\right]+\mathbf{\Xi}_k+\sigma_n^2\ \mathbf{F}_k^H\mathbf{\Psi}^H\left(\mathbf{F}_k^H\mathbf{\Psi}^H\right)^H\right\rangle\boldsymbol{\varpi}_k\end{aligned} \tag{15}$$

Finally, by eliminating terms uninfluenced by $\mathbf{W}$, presented by $\mathbf{Y}$ in (16c), problem $\mathcal{P}_2$ in (17) can be simplified to:

$$\begin{aligned}\mathcal{P}_3\colon\quad&\min_{\mathbf{W}}\quad\mathbf{W}^H\mathbf{A}\mathbf{W}-\mathbb{R}\{2\ \mathbf{C}^H\mathbf{W}\}\\&\ \text{s.t.}\quad \text{C1},\text{C2}\end{aligned} \tag{18}$$

where $\mathbf{D}_b=\mathbf{I}_K\otimes\{(\boldsymbol{\epsilon}_b\ \boldsymbol{\epsilon}_b^H)\otimes\mathbf{I}_M\}$ such that $\boldsymbol{\epsilon}_b\in\mathbb{R}^B$ and $\mathbf{Z}=\mathbf{I}_K\otimes\{\mathbf{G}_b\mathbf{\Psi}^H(\mathbf{G}_b\mathbf{\Psi}^H)^H\}$. Accordingly, the reformulated sub-problem $\mathcal{P}_3$ in (18) can categorized as a standard convex Quadratic Constraint Quadratic Programming (QCQP) problem, since the matrices $\mathbf{A},\ \mathbf{D}_b$ and $\mathbf{Z}$ are identified as positive semi-definite [13]. Accordingly, a feasible solution can be achieved using the primal-dual subgradient (PDS) method [5], [14], to avoid high dimensional matrix inversion of matrix $\mathbf{A}$ introduced by adopting the traditional alternating direction method of multipliers (ADMM) [15].

E. Fixing $(\mathbf{W},\boldsymbol{\rho},\boldsymbol{\varpi})$ and optimizing $\mathbf{\Psi}$:

The active precoders for the RIS to users links are designed for a fixed AP precoding matrix $\mathbf{W}$ and auxiliary variables $\boldsymbol{\rho}$ and $\boldsymbol{\varpi}$. By substituting $\mathbf{h}_k=\sum\limits_{b=1}^{B}\mathbf{h}_{b,k}=\sum\limits_{b=1}^{B}\left(\mathbf{H}_{b,k}^H+\mathbf{F}_k^H\mathbf{\Psi}^H\mathbf{G}_b\right)$ in problem $\mathcal{P}_1$, (12) can be reformulated to:

$$\begin{aligned}\mathcal{P}_4\colon\ &\max_{\mathbf{\Psi}}\ \ \mathcal{R}_2(\mathbf{\Psi},\mathbf{W},\boldsymbol{\rho},\boldsymbol{\varpi})=\sum_{k=1}^{K}\mathbf{q}_k\left(\mathbf{\Psi},\mathbf{W},\ \boldsymbol{\rho},\ \boldsymbol{\varpi}\right)\\&\ \text{s.t.}\quad \text{C2}\end{aligned} \tag{19}$$

where $\mathbf{q}_k\left(\mathbf{\Psi},\mathbf{W},\ \boldsymbol{\rho},\ \boldsymbol{\varpi}\right)$ is given by (15). To simplify the notations, the variables $\mathbf{J}$ and $\mathbf{\Omega}$ are introduced, given by (20) and (21), on the next page, respectively.

Using (20) and (21), problem $\mathcal{P}_4$ in (19) can be reformulated as the following:

$$\begin{aligned}\mathcal{P}_5\colon\quad&\max_{\mathbf{\Psi}}\quad\mathbb{R}\{2\ \mathbf{\Psi}^H\mathbf{J}\}-\mathbf{\Psi}^H\ \mathbf{\Omega}\ \mathbf{\Psi}\\&\quad\text{C2}\colon\ \mathbf{\Psi}^H\ \mathbf{\Sigma}\ \mathbf{\Psi}\leq\mathrm{P_m}\end{aligned} \tag{22}$$

where $\mathbf{\Sigma}=\operatorname{diag}\left(\mathbf{\Sigma}_1,\mathbf{\Sigma}_2,\ldots,\mathbf{\Sigma}_R\right)$ and $\mathbf{\Sigma}_r=\sum\limits_{b=1}^{B}\sum_{j=1}^{K}\mathbf{G}_{b,r}\mathbf{w}_{b,j}\left(\mathbf{G}_{b,r}\mathbf{w}_{b,j}\right)^H+\sigma_n^2\ \mathbf{I}_\mathrm{R}$

Finally, each variable is updated separately until the WSR converges. Moreover, $\boldsymbol{\rho}$ and $\boldsymbol{\varpi}$, are updated using (13) and (14), respectively. While $\mathbf{W}$ and $\mathbf{\Psi}$ are updated by solving (18) and (22), respectively. Similar to the aforementioned reasons for (18), eq. (22) can also be solved using PDS to avoid high dimensional matrix inversion of $\mathbf{\Sigma}$.

VI. Numerical Results and discussion

In this section, the proposed joint precoding algorithm is evaluated for a multi-user CF-MIMO system, aided by either active or passive RIS. The values of the simulation parameters are summarized in Table I. Additionally, as an initialization to the alternating algorithm, $\mathbf{W}$ and $\mathbf{\Psi}$ are initialized by unity powers and random phases and the user weights are all set to $\eta_k=\eta=1$. The results are achieved by taking the average of 30 channel realizations. Finally, the system transmission power is denoted by P such that $P_b=0.9*P$ and $P_R=0.1*P$ are the maximum transmission powers for each AP and for all RIS, respectively.

A. Simulation paramaters and setup

To analyze the achieved results, 5 schemes are considered:

- **Without RIS:** This scenario represents a benchmark conventional distributed MIMO system. Accordingly, all the system power is allocated to the AP-Users links
- **Passive RIS with no DL:** The performance of the passive RIS when the DL between the APs and the users is completely blocked, using the joint precoding algorithm in [5].
- **Passive RIS:** The performance of the passive RIS when a DL between the APs and the users can be established, using the joint precoding algorithm in [5].
- **Active RIS with no DL:** The performance of the active RIS which add an amplification gain prior to signal reflection, when the DL between the APs and the users is completely blocked.

$$\mathbf{J} = 2\sum_{k=1}^{K} \mu_k \boldsymbol{\varpi}_k \mathbf{F}_k^H \left(\sum_{b=1}^{B} \mathbf{G}_b \mathbf{w}_{b,k}\right) - \sum_{k=1}^{K} \boldsymbol{\varpi}_k^H \mathbf{F}_k^H \left[\sum_{b=1}^{B} \mathbf{G}_b \left(\sum_{j=1}^{K} \mathbf{w}_{b,j}\mathbf{w}_{b,j}^H\right) \mathbf{H}_{b,k} + \mathbf{H}_{b,k}^H \left(\sum_{j=1}^{K} \mathbf{w}_{b,j}\mathbf{w}_{b,j}^H \mathbf{G}_b^H\right)\right] \mathbf{F}_k \boldsymbol{\varpi}_k \tag{20}$$

$$\boldsymbol{\Omega} = \sum_{k=1}^{K} \boldsymbol{\varpi}_k^H \left(\sigma_n^2\, \mathbf{F}_k^H \mathbf{F}_k\right) \boldsymbol{\varpi}_k + \sum_{k=1}^{K} \boldsymbol{\varpi}_k^H \left[\mathbf{F}_k^H \left\langle \sum_{b=1}^{B} \mathbf{G}_b \left(\sum_{j=1}^{K} \mathbf{w}_{b,j}\mathbf{w}_{b,j}^H\right) \mathbf{G}_b^H \right\rangle \mathbf{F}_k\right] \boldsymbol{\varpi}_k \tag{21}$$

TABLE I
SIMULATION PARAMETERS

Parameter	Description	Value
B	Number of APs, of height 3 m	5
M	Number of AP antennas	3
R	Number of RISs, of height 6 m	2
N	Number of RIS elements	200
K	Number of users, of height 1.5 m	4
U	Number of user antennas	2
R_D	Radius of user distribution circle	1 m
D	Center of user distribution circle	65m, when fixed.
σ_n^2	AWGN of the user received signal	-70 dBm
σ_v^2	Noise power due to active RIS	-70 dBm
κ	Rician factor	20
τ_{AP-R}	Path-loss exponent for the AP to RIS link	2.2
τ_{AP-U}	Path-loss exponent for the AP to users link	2.2
τ_{R-U}	Path-loss exponent for the RIS to users link	2.2

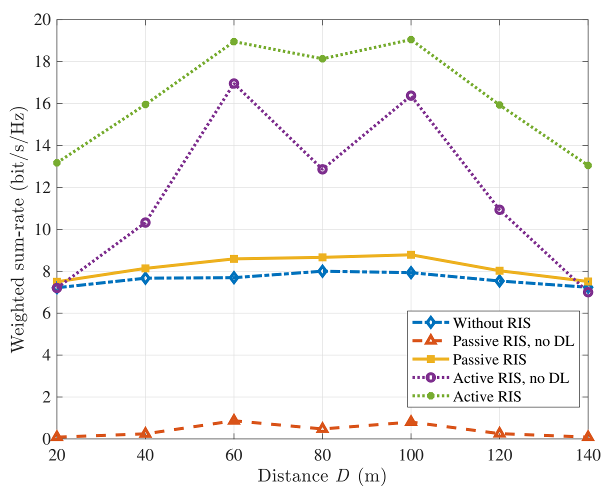

Fig. 2. Users' distribution center point D vs. WSR for $P = 0$ dBm and $N = 200$.

- **Active RIS:** The performance of the active RIS which add an amplification gain prior to signal reflection, when a DL between the APs and the users can be established.

In Fig.2, the WSR is plotted vs. D. The active RIS schemes introduce a significant WSR gain over the passive RIS and without RIS schemes, unlike the passive RIS scheme which shows a minimal improvement. Two major peaks are shown at $D = 60$ m, 100 m for all the schemes incorporating RIS. The reason for those peaks is that the users at a close proximity to the RIS experience an improved SINR due to the signals reflected by the RIS. In particular, at $D = 60$, the WSR of the active RIS increase from 1 bit/s/Hz to 17 bits/s/Hz and from 8.5 bits/s/Hz to 19 bits/s/Hz for the scenarios when the DL is blocked and when a DL exists, respectively.

In Fig. 3, the WSR is plotted vs. P. A WSR enhancement is depicted as the transmit power P increases for all 5 scenarios. This is due to the fact that higher values of P result in stronger reflected signals by the RIS and thus an improved SINR at the users. Moreover, the passive RIS scheme shows a minimal performance enhancement over the without RIS scheme due to the multiplicative fading effect. For $P = 20$ dBm, the active RIS scheme incorporating a DL shows an enhancement of approximately 37% over the without RIS scheme. On the other hand, the passive RIS scheme introduces an enhancement of only 2%. However, for the scenario when a DL is blocked, an enhancement of approximately 236% is introduced by the active RIS scheme over the passive RIS scheme. Accordingly, the active RIS leads to a more significant performance enhancement when the DLs between the APs and users are completely blocked.

Due to the high dimensional channels, channel estimation for CF aided MIMO network is considered very challenging. Thus, we accommodate for the CSI error δ by introducing a zero mean Gaussian distributed random variable such that the estimated channel is given by $\hat{h} = h + e$ where h and e denote the real channel and the estimation error, respectively. Thus, $e \sim \mathcal{CN}\left(0, \sigma_e^2\right)$, where the variance representing the error power, satisfies $\sigma_e^2 \triangleq \delta\, |h|^2$. Fig. 4 shows a performance degradation as δ increases. For instance, when $\delta = 0.4$ and thus the error power is 40% of the channel gain, the WSR is reduced by $33\%, 38\%, 30\%$ for the scenarios with without RIS, passive RIS and active RIS, respectively. Thus, the active RIS scheme is the most robust.

In Fig.5, the WSR is plotted vs. N for $P = 0$ dBm. The figure shows that the WSR increases as the number of RIS elements increases. However, increasing N increases the system complexity due to the high dimensional matrices. Accordingly, N must be chosen reasonably to achieve a trade off between the performance gain and the system complexity. In particular, for $N = 200$, the WSR increases from approximately 8 bits/s/Hz without RISs used to 9 bits/s/Hz and 13 bits/s/Hz for passive and active RIS in the presence of a DL, respectively.

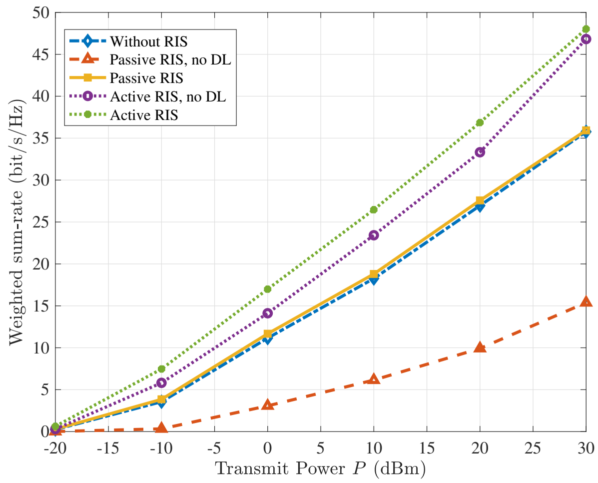

Fig. 3. Transmission power P vs. WSR for $N = 200$.

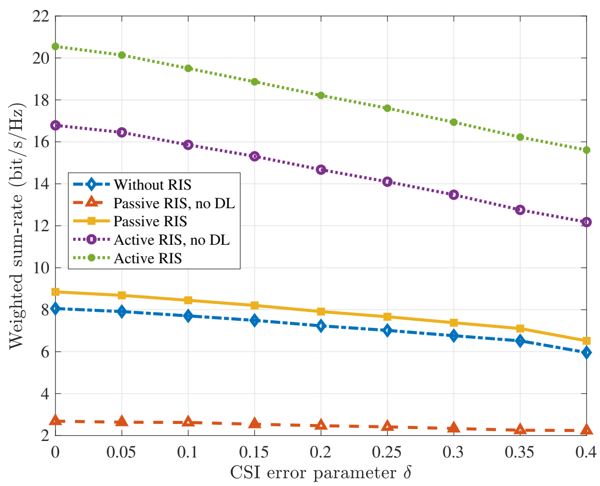

Fig. 4. CSI error δ vs. WSR for $P = 0$ dBm and $N = 200$.

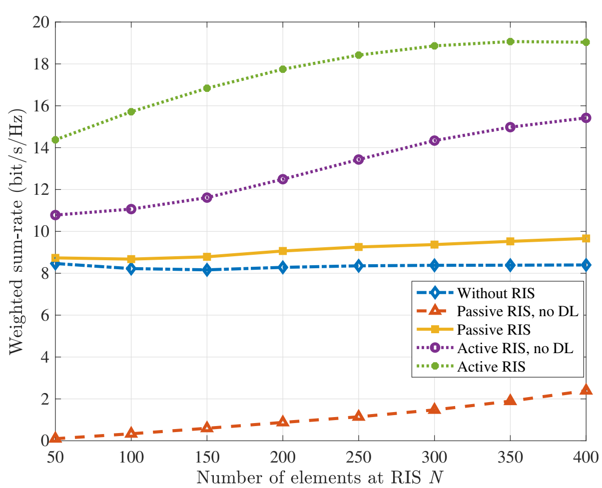

Fig. 5. Number of RIS elements N vs. WSR for $P = 0$ dBm.

VII. Conclusion and Future Work

The main objective of this paper is to investigate the performance gains introduced by active RIS over passive RIS. A joint precoding technique is implemented, aiming to maximize the WSR subject to AP and RIS transmit power constraints. Results show that active RIS constitute to a significant WSR gain in comparison to passive RIS. For future work, we recommend investigating a more practical channel model in the presence of CSI error. Furthermore, hybrid RIS can also be implemented to achieve a tradeoff between the energy efficiency and the performance gain introduced by the RIS.

References

[1] Hien Quoc Ngo, Alexei Ashikhmin, Hong Yang, Erik G Larsson, and Thomas L Marzetta. Cell-free massive mimo versus small cells. *IEEE Transactions on Wireless Communications*, 16(3):1834–1850, 2017.

[2] Jiayi Zhang, Shuaifei Chen, Yan Lin, Jiakang Zheng, Bo Ai, and Lajos Hanzo. Cell-free massive mimo: A new next-generation paradigm. *IEEE Access*, 7:99878–99888, 2019.

[3] Manijeh Bashar, Kanapathippillai Cumanan, Alister G Burr, Hien Quoc Ngo, Erik G Larsson, and Pei Xiao. Energy efficiency of the cell-free massive mimo uplink with optimal uniform quantization. *IEEE Transactions on Green Communications and Networking*, 3(4):971–987, 2019.

[4] Miguel Dajer, Zhengxiang Ma, Leonard Piazzi, Narayan Prasad, Xiao-Feng Qi, Baoling Sheen, Jin Yang, and Guosen Yue. Reconfigurable intelligent surface: Design the channel–a new opportunity for future wireless networks. *Digital Communications and Networks*, 8(2):87–104, 2022.

[5] Zijian Zhang and Linglong Dai. A joint precoding framework for wideband reconfigurable intelligent surface-aided cell-free network. *IEEE Transactions on Signal Processing*, 69:4085–4101, 2021.

[6] Trinh Van Chien, Hien Quoc Ngo, Symeon Chatzinotas, Marco Di Renzo, and Björn Ottersten. Reconfigurable intelligent surface-assisted cell-free massive mimo systems over spatially-correlated channels. *IEEE Transactions on Wireless Communications*, 21(7):5106–5128, 2021.

[7] Yuhong Wang and Jingyi Peng. Energy efficiency fairness of active reconfigurable intelligent surfaces-aided cell-free network. *IEEE Access*, 2023.

[8] Emil Björnson and Luca Sanguinetti. Cell-free versus cellular massive mimo: What processing is needed for cell-free to win? In *2019 IEEE 20th International Workshop on Signal Processing Advances in Wireless Communications (SPAWC)*, pages 1–5. IEEE, 2019.

[9] Zijian Zhang, Linglong Dai, Xibi Chen, Changhao Liu, Fan Yang, Robert Schober, and H Vincent Poor. Active ris vs. passive ris: Which will prevail in 6g? *arXiv preprint arXiv:2103.15154*, 2021.

[10] Jean-François Bousquet, Sebastian Magierowski, and Geoffrey G Messier. A 4-ghz active scatterer in 130-nm cmos for phase sweep amplify-and-forward. *IEEE Transactions on Circuits and Systems I: Regular Papers*, 59(3):529–540, 2011.

[11] Kaiming Shen and Wei Yu. Fractional programming for communication systems—part i: Power control and beamforming. *IEEE Transactions on Signal Processing*, 66(10):2616–2630, 2018.

[12] Werner Dinkelbach. On nonlinear fractional programming. *Management science*, 13(7):492–498, 1967.

[13] Stephen Boyd, Stephen P Boyd, and Lieven Vandenberghe. *Convex optimization*. Cambridge university press, 2004.

[14] Yurii Nesterov. Primal-dual subgradient methods for convex problems. *Mathematical programming*, 120(1):221–259, 2009.

[15] Stephen Boyd, Neal Parikh, Eric Chu, Borja Peleato, Jonathan Eckstein, et al. Distributed optimization and statistical learning via the alternating direction method of multipliers. *Foundations and Trends® in Machine learning*, 3(1):1–122, 2011.